

The Degradation of a Pulsed Neutron Beam by Inelastically Scattering Collimators.

Colin G. Windsor

Materials Physics and Metallurgy Division, B 418 AERE Harwell . OX11 0RA.

Summary. Pulsed neutron beams for neutron scattering experiments are degraded by scattering from the collimators used to define the beam. A simple analytic theory including down-scattering from the collimators is used to estimate the beam-born background from the circular iris collimators usually employed. The results are used to give guidelines for the practical design of collimators.

1. Introduction

The dominant contribution to the neutron scattering background in most neutron scattering experiments comes from neutrons within the instruments's own beam. Some of the possible contributions to this are listed in figure 1. A simple collimator is assumed consisting of circular irises in a cylindrical tube. Consider some of the contributions to the background measured at the point P, just outside the geometric penumbra of the beam.

- (i) The transmitted background is the term frequently calculated. These are the neutrons which have not suffered scattering so that their energy is not degraded from that calculated simply from their time of flight.
- (ii) The primary scattered background has been intensively studied by algebraic and Monte Carlo methods (1,2). However, a vital feature often neglected is that the scattering processes are inelastic. For higher energy neutrons, the tendency is for down-scattering, so that the scattered velocity v_1 is less than the incident velocity v_0 . A neutron arriving at a flight time corresponding to a direct velocity v_d may therefore have left the moderator at a higher or lower neutron energy depending on whether the scattering collimator was nearer the source, or nearer the sample.
- (iii) Higher order contributions can arise from neutrons scattered successively from two surfaces. from scattering from one surface followed by transmission through an iris, and so on.

The primary scattered contribution (ii) is the object of special study in this paper. To make analytic progress, the scattering collimator is assumed to be several scattering lengths thick so that its surface can be considered as a moderator.

2. The inelastic scattering from a single collimator ring.

Figure 2 illustrates the simple geometry to which the inelastic theory is applied. A point moderator M emits neutrons with a slowing down spectral flux as a function of wavelength λ given by (3)

$$n_0(\lambda) \delta\lambda \delta\Omega = \frac{B_0}{\lambda^{1+2\alpha_0}} \delta\lambda \delta\Omega. \quad 1.$$

B_0 is a measure of the moderator flux per unit time, per unit wave length per steradian. α_0 is the buckling term, with a value from zero to 0.15 for pulsed source moderators, describing the surface losses from the moderator during slowing down. A point sample S receives neutrons at a distance L from the moderator. The direct flux at the sample between the elastic wavelength λ_d and $\lambda_d + \delta\lambda_d$ is given by

$$n_d(\lambda_d) \delta\lambda_d = \frac{B_0}{\lambda_d^{1+2\alpha_0}} \frac{\delta\lambda_d}{4\pi L^2} \quad 2.$$

per unit area per unit time. All background fluxes in this paper will be presented as a background fraction with respect to this direct flux.

Consider next the indirect beam scattered from the inner surface of the iris collimator shown. The iris surface is of radius r , length l and centred at a distance x from the moderator. The solid angle of the iris front aperture seen by the source is

$$\Omega_0 = \frac{\pi r^2}{4\pi(x-l/2)^2}. \quad 3.$$

The solid angle Ω_0 is unchanged for an extended moderator lying on the sphere shown dashed in figure 2. It follows that if moderator extent is small compared with x , equation 3 applies equally for an extended moderator. The solid angle from the iris back surface Ω_1 is similar with $x+l/2$ in the denominator giving for the incident solid angle subtended by the inner surface.

$$\Delta\Omega_0 = \Omega_0 - \Omega_1 = \frac{r^2 x l}{2[x^2 - (l/2)^2]^2} \doteq \frac{r^2 l}{2x^3} \quad 4.$$

provided that $x > l/2$. The area of the iris inner surface is $2\pi r l$, so that the mean flux of neutrons over the inner surface per unit area between wavelengths λ_0 and $\lambda_0 + \delta\lambda_0$ is

$$n_0(\lambda_0) \delta\lambda_0 = \frac{B_0}{\lambda_0^{1+2a}} \frac{r^2 l}{2x^3} \frac{\delta\lambda_0}{2\pi r l} \quad 5.$$

Of these neutrons a fraction $A(\lambda_0)$, the albedo, will be scattered back from the same surface of the collimator (3). If the collimator is several scattering lengths thick, the scattered neutrons will emerge equally in all directions. Others may be absorbed and still others scattered further within the material. $A(\lambda_0)$ can be found by experiment or calculated from the scattering cross-sections. It varies from about 15% for a totally coherent scatterer such as polyethylene, though 12 % for iron, to 0.13% for boron carbide.

During the scattering process occurring in the iris, slowing down of the neutrons will be occurring so that the emitted neutrons will be at a generally longer wavelength $\lambda_1 > \lambda_0$. This process occupies some moderation time t_m shown by experiment and theory to be proportional to wavelength (4). The process is exactly analogous to the time delay during slowing down neutrons in the moderator where neutrons emitted at a wavelength λ_0 experience a time delay

$$t_m = C_0 \lambda_0$$

The constant C_0 is around $10 \mu\text{s}\text{\AA}^{-1}$ for hydrogenous materials, but increases to $80 \mu\text{s}\text{\AA}^{-1}$ for heavier elements such as iron. The time delay in the shielding material incurred by slowing neutrons down from wavelength λ_0 to wavelength λ_1 will be similar but with a different time constant C_1

$$\Delta t_m = C_1(\lambda_1 - \lambda_0) \quad 6.$$

Figure 3 illustrates the spectrum of neutrons emitted by incident neutrons of wavelength λ_0 . Once again the epithermal distribution of equation 1 is assumed, but with a changed buckling constant α_1 likely to be closer to zero for a thick semi-infinite iris. The total number of emitted neutrons $n_1(\lambda_1)$ from all wavelengths from λ_0 to ∞ must be equal to the number incident $n_0(\lambda_0)\delta\lambda_0$ attenuated by $A(\lambda_0)$.

$$n_0(\lambda_0) \delta\lambda_0 A(\lambda_0) = \int_{\lambda_0}^{\infty} n_1(\lambda_1) d\lambda_1 = \int_{\lambda_0}^{\infty} \frac{B_1}{\lambda_1^{1+2\alpha_1}} d\lambda_1 = \frac{B_1}{2\alpha_1 \lambda_0^{2\alpha_1}}. \quad 7.$$

This expression defines the constant B_1 in the emitted neutron spectrum. The number of neutrons emitted from the inner surface of the collimator within the band λ_1 to $\lambda_1 + \delta\lambda_1$ from incident neutrons λ_0 to $\lambda_0 + \delta\lambda_0$ is therefore

$$n_1(\lambda_0, \lambda_1) \delta\lambda_0 \delta\lambda_1 = \frac{2\alpha_1 \lambda_0^{2\alpha_1}}{\lambda_1^{1+2\alpha_1}} A(\lambda_0) \frac{B_0}{\lambda_0^{1+2\alpha_0}} \frac{r^2 l}{2x^3} \frac{\delta\lambda_0}{2\pi r l} \delta\lambda_1. \quad 8.$$

If these neutrons are emitted isotropically, the number reaching the sample position will be reduced by the solid angle of the collimator inner surface as seen by the sample $\Delta\Omega_1$. This will be equation 4 with x replaced by $L-x$,

$$n_s(\lambda_0, \lambda_1) \delta\lambda_0 \delta\lambda_1 = \frac{2\alpha_1 \lambda_0^{2\alpha_1}}{\lambda_1^{1+2\alpha_1}} A(\lambda_0) \frac{B_0}{\lambda_0^{1+2\alpha_0}} \frac{r^2 l}{2x^3} \frac{r^2 l}{2(L-x)^3} \frac{\delta\lambda_0 \delta\lambda_1}{2\pi r l}. \quad 9.$$

Let us next consider the flight times of the neutrons. The direct neutrons will have a flight time over the path L of

$$t_d = \left(\frac{mL}{h} + C_0\right) \lambda_d. \quad 10.$$

The constant $\frac{m}{h}$ is equal to 0.3956 for t in μ s, L in cm and λ in \AA . This flight time is illustrated by the dashed line in figure 4. The inelastically scattered neutrons have a total flight time consisting of an initial delay in the moderator C_0 , a flight time to the collimator $m\lambda_0/h$, a time delay during moderation $C_1(\lambda_1 - \lambda_0)$, and a flight time from collimator to sample $m(L-x)\frac{\lambda_1}{h}$, making a total

$$t(\lambda_0, \lambda_1) = \left(\frac{mx}{h} + C_0 - C_1\right)\lambda_0 + \left(\frac{m(L-x)}{h} + C_1\right)\lambda_1 = t_d \quad 11.$$

The inelastic background to be calculated is the ratio between the indirect and direct neutron fluxes arriving at the sample in the same time interval between t_d and $t_d + \delta t_d$. For direct neutrons this corresponds to neutrons of wavelengths λ_d to $\lambda_d + \delta\lambda_d$. Differentiating equation 10, and using equation 2 this direct flux is seen to be

$$n_d(\lambda_d)\delta\lambda_d = \frac{B_0}{\lambda_d^{1+2\alpha_0}} \frac{1}{\frac{mL}{h} + C_0} \frac{\delta t_d}{4\pi L^2}. \quad 12.$$

The inelastically scattered neutron flux is found by intergrating over all incident and scattered wavelengths with the constraint that the total flight time falls between t_d and $t_d + \delta t_d$. Figure 4 illustrates such a set of scattering possibilities. An option is to equate δt_e with the finite δt_1 corresponding to the wavelength spread $\delta\lambda_1$ of the scattered neutrons. The incident wavelength spread $\delta\lambda_0$ is made infinitesimal and incorporated into an integral over λ_0 . From equation 11 the scattered wavelength λ_1 corresponding to a given total time t_d and wavelength λ_0 is given by

$$\lambda_1 = \frac{(L + C_0 h/m)\lambda_d - (x + C_0 h/m - C_1 h/m)\lambda_0}{L - x + C_1 h/m}. \quad 13.$$

At a fixed λ_0 the relationship between δt_d and $\delta\lambda_1$ is given by differentiating as

$$\delta\lambda_1 (L - x + C_1 h/m) = \delta t_d h/m. \quad 14.$$

The number of neutrons reaching the sample between times t_d and $t_d + \delta t_d$ is then

$$\int_0^{\lambda_d} n_s(\lambda_0, \lambda_1) d\lambda_0 \delta\lambda_1 = \frac{\alpha_1 B_0 r^3 l}{4\pi x^3 (L-x)^3} \int_0^{\lambda_d} \frac{A(\lambda_0) \lambda_0^{2\alpha_1} d\lambda_0}{\lambda_0^{1+2\alpha_0} \lambda_1^{1+2\alpha_1}} \frac{\delta t_d h/m}{(L-x + C_1 h/m)}. \quad 15.$$

Comparing with equation 12 gives the inelastically scattered fraction. The integral is cast in dimensionless terms with

$$\xi = \frac{x}{L}, \quad \rho = \frac{r}{L}, \quad \mu = \frac{l}{2L}, \quad \nu = \frac{\lambda_0}{\lambda_d}, \quad \delta_0 = C_0 \frac{h}{mL} \quad \text{and} \quad \delta_1 = C_1 \frac{h}{mL}. \quad 16.$$

Writing it in the form of the albedo A , a geometric term G and the inelastic integral I gives

$$F = A G I$$

with

$$G = \frac{r^3 l L^2}{x^3 (L-x)^3} = \frac{\rho^3 \mu}{\xi^3 (1-\xi)^3} \quad 17.$$

and

$$I = \alpha_1 (1 + \delta_0)(1 - \xi + \delta_1)^{2\alpha_1} \int_0^1 \frac{dv}{v^{1+2\alpha_0-2\alpha_1} [1 + \delta_0 - (\xi + \delta_0 - \delta_1)v]^{1+2\alpha_1}}. \quad 18.$$

An alternative integral is obtained if the integration is performed over scattered wavelengths λ_1 with $\delta\lambda_0$ scaled to give the chosen time interval δt_d . Putting $\varepsilon = \frac{\lambda_1}{\lambda_d}$ as the variable gives the equivalent integral

$$I = \alpha_1 (\xi + \delta_0 - \delta_1)^{2\alpha_0-2\alpha_1} \int_1^{(1+\delta_0)/(1-\xi+\delta_1)} \frac{d\varepsilon}{[1 + \delta_0 - (1-\xi+\delta_1)\varepsilon]^{1+2\alpha_0-2\alpha_1} \varepsilon^{1+2\alpha_1}} \quad 15.$$

A number of interesting features can be noted from evaluating either integral numerically

- (i) The geometric term G of equation 17 shows that scattering centres close to either the moderator or sample give a relatively large contribution and so should be used with caution.
- (ii) Apart from the albedo term, the scattering fraction is independent of the incident neutron energy in this approximation.
- (iii) Figure 5(i) shows the integral evaluated for negligible moderation delay $\delta_0 = \delta_1 = 0$, $\alpha_0 = 0$, and a rapid collimator slowing down $\alpha_1 = 0.5$. The largest contribution to the integral is close to the direct wavelength λ_d . The inelastic integral becomes close to unity, indeed it is exactly unity for the conditions of figure 5(i).
- (iv) Figure 5(ii) shows the integral for the more practical case of the moderator buckling $\alpha_0 = 0.15$ and the collimator buckling $\alpha_1 = 0.05$, with $\delta_0 = \delta_1 = 0$. For this example the inelastic integral is appreciably larger than unity. The largest contribution to the integral comes from the shortest wavelengths, and for $\alpha_0 > \alpha_1$ the integral can in principle diverge. In practice the $\frac{1}{\lambda^{1-\alpha_0}}$ divergence cannot continue indefinitely and the integral remains finite. The conclusion remains that any moderating material can become a serious background source if near either the target or the sample area.
- (v) The inclusion of a moderation time delay causes a further increase in the value of the inelastic integral. Figure 6(iii) shows its value for negligible moderator delay $\delta_0 = 0.0$, but with appreciable moderation delay in the shielding $\delta_1 = 0.25$. The time-distance plot shows the effect for a moderator to collimator distance $L - x$ equal to the moderation effective moderation distance $C_1 h/m$. The scattered neutron energy is the same for any incident neutron energy leading to the appearance of ghost source near the true moderator.

3. The complete collimator

Returning to figure 1, let us consider the conclusions for good collimator design suggested by the present calculations. Numerical estimates will be considered in another report. The aim should be to reduce the background fraction F given roughly by observed

counts at P divided by incident counts at S to the values of order 10^{-6} given by a good reactor small angle spectrometer.

- (i) An iris transmission of this order is easy to achieve, at any rate below 1 ev, by a mere 1 cm thickness of boron carbide. Thus it is likely to be the collimator scattering which dominates the observed background.
- (ii) The scattering surfaces seen by both moderator and sample area are the main subject of the paper. This surface is clearly reduced by splitting the collimator into a series of relatively thin irises of radius r_i , length l_i at positions x_i . The primary iris scattering function is

$$F = \sum_i \frac{r_i^3 l_i L^2 A_i I_i}{2x_i^3 (L-x_i)^3} \quad 20.$$

Consider a 10 m long, 10 cm diameter collimator with irises 10 cm long. The geometric term is only 0.04×10^{-6} for an iris at 5 m but rises to 0.85×10^{-6} at 1 m or 9 m close to the moderator or sample, and to 83×10^{-6} at 20 cm from the moderator or sample. Clearly collimators placed at these positions must be designed with great care, for example by ensuring low albedo by using low hydrogen content B₄C shielding.

- (iii) Double scattering processes are potentially almost as large since, as indicated in figure 6, the bright and visible surfaces on adjacent irises can be of much larger area than the edges of the irises. Figure 7 illustrates the calculation of the solid angles subtended by these areas at the moderator and sample

$$\delta\Omega_0 = \frac{\pi(r_i^2 - r^2)}{x_i^2} \quad \delta\Omega_1 = \frac{\pi(r_j^2 - r^2)}{(L-x_j)^2}.$$

The scattering fraction is seen to have had a contribution

$$\delta\Omega_0 \frac{A_i}{4\pi} \frac{1}{(x_i - x_j)^2} \delta\Omega_1 \frac{A_j}{4\pi}$$

giving for the overall geometric scattering fraction

$$G = \sum_i \sum_{j < i} \frac{r^4 (x_i^2 - x_j^2) ((L-x_i)^2 - (L-x_j)^2) L^2}{16x_i^4 (L-x_j)^4 (x_i - x_j)^2} \quad 21.$$

and depends on the square of the albedo, and also on a double inelastic integral which we have not evaluated. To estimate this term consider a single pair of surfaces between two adjacent irises at x_i and x_j -S. This term is

$$G_{ij} = \frac{r^4 (2x_i S - S^2) (2(L-x_i)S - S^2) L^2}{16x_i^4 (L-x_j)^4} \quad 22.$$

With the reasonable approximation that the separation S is small compared with x_i or $L-x_j$ this becomes independent of S giving

$$G_{ij} = \frac{r^4 L^2}{4x_i^3 (L-x_j)^3} \quad 23.$$

The equation closely resembles equation 20 and gives terms of comparable size. It follows that both inside and outside surfaces of the iris should be covered with low albedo surfaces.

- (iv) The outer region of the collimator must not be neglected. Neglecting the positional dependence of the albedo and inelasticity integral of a collimator from x_1 to x_2 gives a scattering fraction

$$F = A I \frac{r^3}{2L^3} \left[\frac{1}{2\xi^2(1-\xi^2)} + \frac{2}{\xi^2(1-\xi)} - \frac{3(2\xi+1)}{\xi^2} + 6 \ln \frac{\xi}{1-\xi} \right]_{x_1/L}^{x_2/L}. \quad 24.$$

This geometry of collimator has been investigated by Soper(5). This fraction can become very serious if the collimator extends close to moderator or sample. For example for a collimator extending from $x_1=100$ cm to $x_2=900$ cm. for a 10 cm diameter 10 m long collimator the geometric scattering fraction is 8.2×10^{-6} . Inelastic effects can be very important here, as thin boron carbide irises do little to prevent fast neutrons entering this region. Although slow neutrons emitted by the collimator are not directly visible near the sample, they may easily be scattered off an iris surface as in the previous section. The solution is to make the outer region of the collimator from absorbing materials with a low albedo surface.

References

- (1) G M Vineyard Phy Rev 96 (1954) 93
- (2) V F Sears Adv Phys 24 (1975) 1
- (3) C G Windsor Pulsed Neutron Scattering, Taylor and Francis, London, 1981
- (4) K H Beckurts and J Wirtz Neutron Physics Springer Verlag, Berlin, 1964
- (5) A K Soper, Nucl Inst Meth 212 (1983) 337

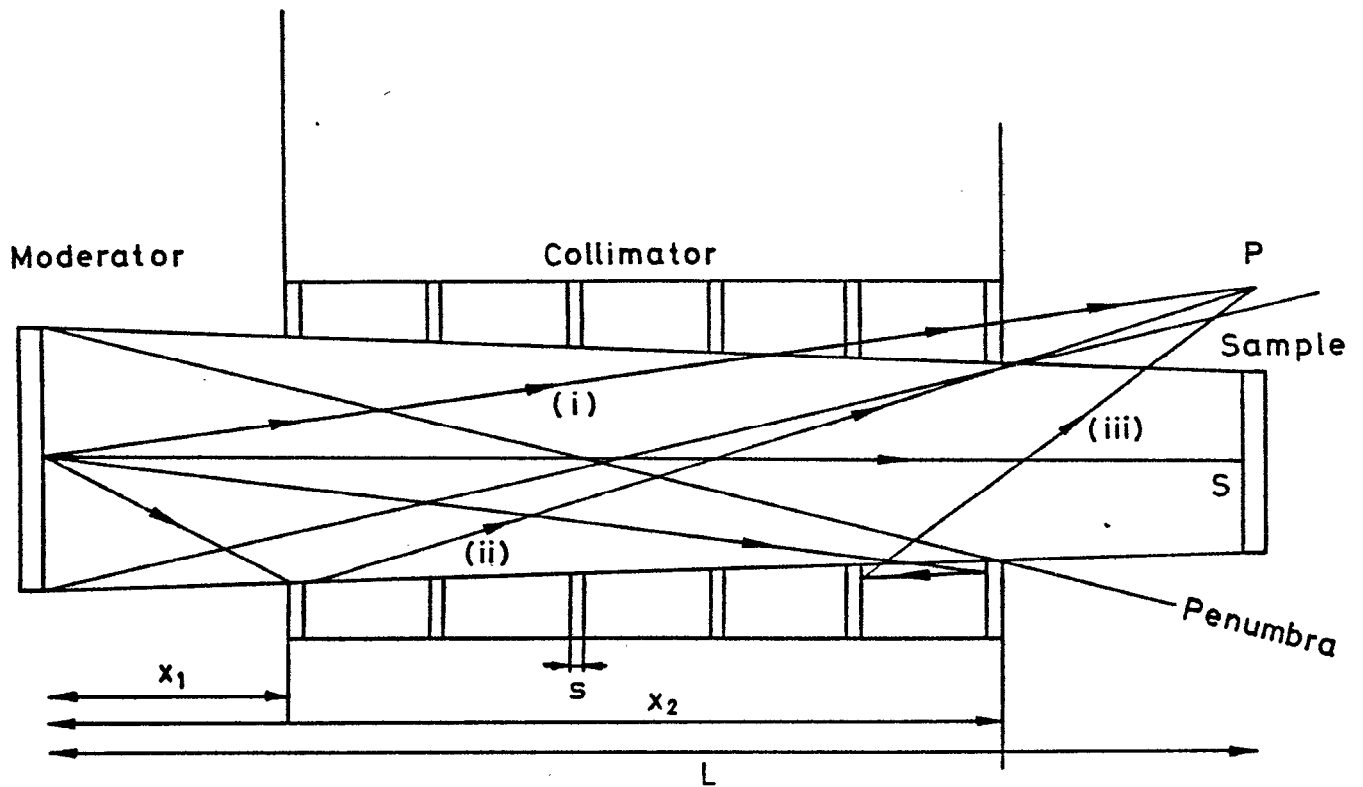


Figure 1. The contributions to the neutron background at a point P just outside the geometric penumbra of the collimator. (i) neutrons transmitted by the collimator (ii) neutrons scattered by the collimator (iii) neutrons doubly-scattered or scattered and transmitted.

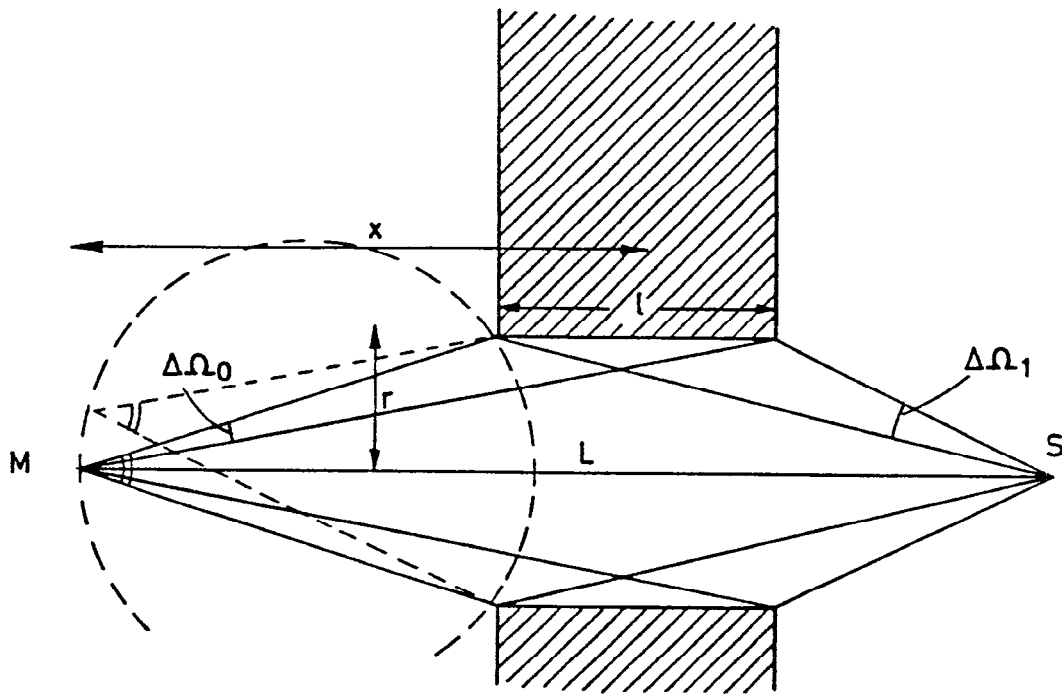


Figure 2. Scattering from a circular iris collimator. A geometric term depends on the incident and scattered solid angles $\Delta\Omega_0$, $\Delta\Omega_1$. An inelasticity term depends on slowing down properties of the moderator and iris.

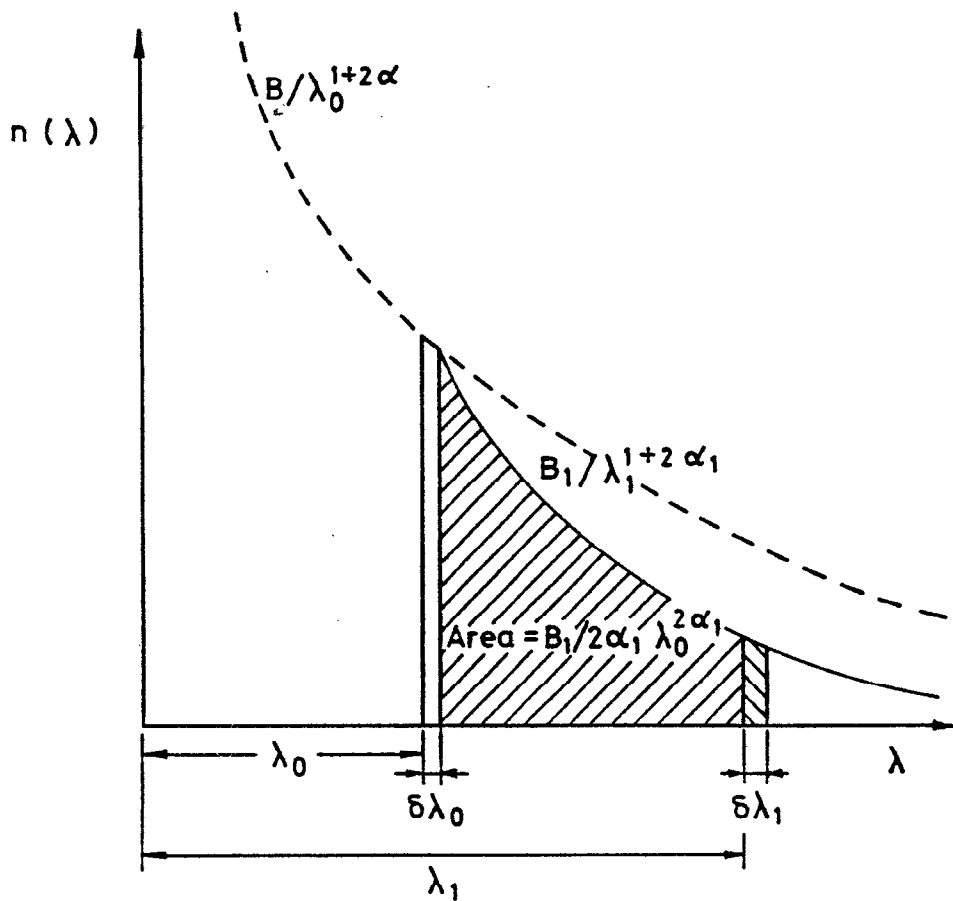


Figure 3. The flux incident on a collimator between wavelengths λ_0 and $\lambda_0 + \delta\lambda_0$, is assumed to be partly re-admitted over a range of wavelengths λ_1 from λ_0 to infinity with a slowing down distribution $B_1/\lambda_1^{1+2\alpha_1}$.

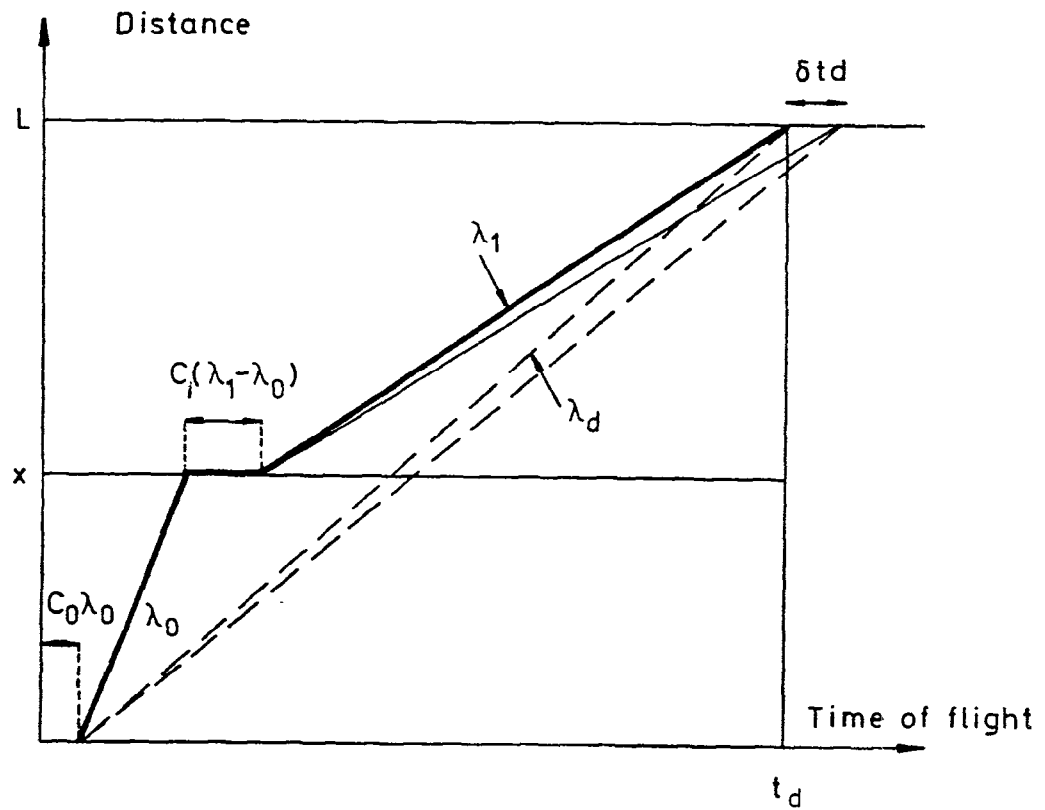


Figure 4. The time/distance diagram for inelastically scattering collimators. Direct neutrons arrive between times t_d and $t_d + \delta t_d$. The set of inelastic neutrons is considered which travel at any wavelength λ_0 to the collimator at x , and then travel to arrive at time t_d with wavelength λ_1 including a moderation time delay proportional to $C_0 \lambda_0$ and a delay due to moderation in the shielding proportional to $C_1 (\lambda_1 - \lambda_0)$.

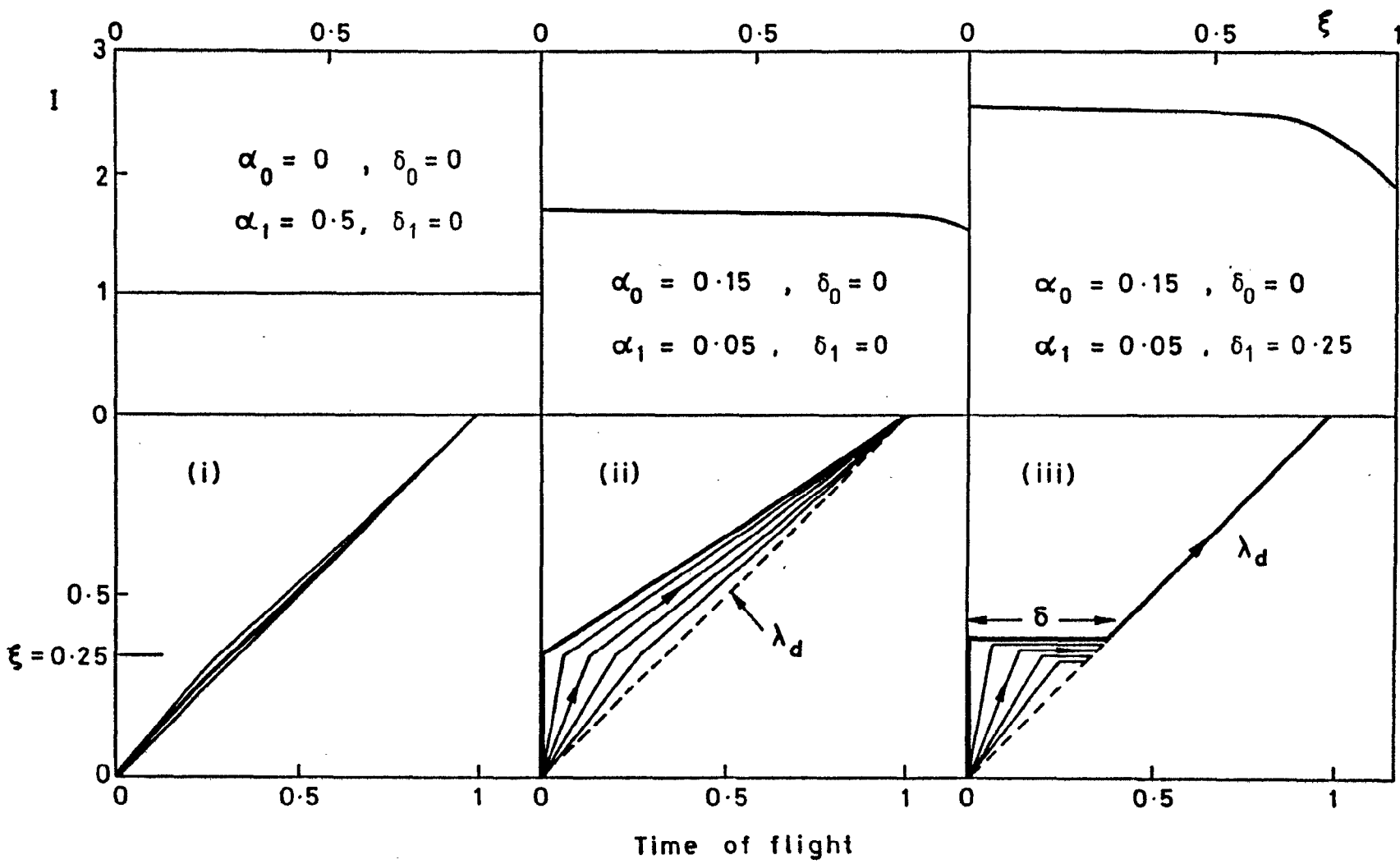


Figure 5. The inelastic integral I evaluated as a function of position down the collimator ξ , with corresponding time/distance diagrams for $\xi=1/3$. (i) if the collimator buckling is relatively large most scattering is elastic and $I = 1$. (ii) if the moderator buckling exceeds the collimator buckling the integral rises and becomes dominated by incident fast neutrons (iii) with moderation delay in the iris material $\delta_1 = \xi$ the inelastic integral increases, and can give the same scattered energy for all incident energies.

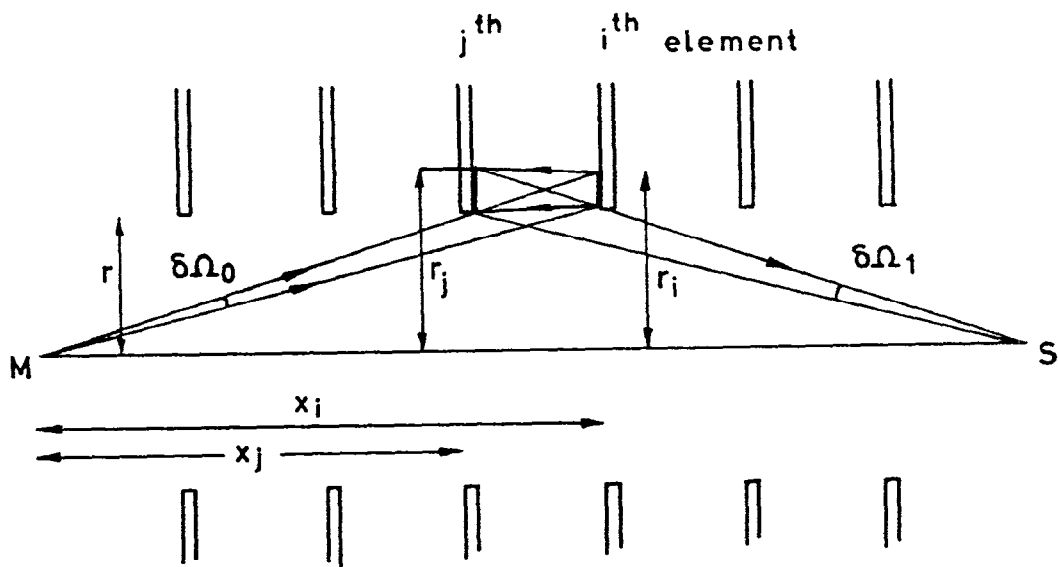


Figure 6. Double scattering from a pair of collimator irises. The *bright* area of radius $r_i = rx_i/x_j$ on the i^{th} iris, reflects back to a *visible* area of radius $r_j = r(L-x_i)/(L-x_j)$ on the j^{th} iris. The increase in these areas with increasing separation between irises exactly cancels the decrease in scattered neutron intensity arising from the inverse square law.